Robotica (2010) volume 28, pp. 909–917. © Cambridge University Press 2009
doi:10.1017/S0263574709990749

A novel five-degrees-of-freedom decoupled robot

Jaime Gallardo-Alvarado†,*, Horacio Orozco-Mendoza† and José M. Rico-Martínez‡

†*Department of Mechanical Engineering, Instituto Tecnológico de Celaya, Av. Tecnológico y A. García Cubas, 38010 Celaya, GTO, México*
‡*Department of Mechanical Engineering, FIMEE, Universidad de Guanajuato, Salamanca – Valle de Santiago km 3.5 Salamanca, GTO, México*

(Received in Final Form: November 11, 2009. First published online: December 23, 2009)

SUMMARY
In this work a new nonoverconstrained redundant decoupled robot, free of compound joints, formed from three parallel manipulators, with two moving platforms and provided with six active limbs connected to the fixed platform, called LinceJJP, is presented. Interesting applications such as multi-axis machine tools with parallel kinematic architectures, solar panels, radar antennas, and telescopes are available for this novel spatial mechanism.

1. Introduction

Since the pioneering contributions of Gough[1,2] and Stewart[3] a tire testing machine and a flight simulator, respectively, where both inventions are based on parallel mechanical devices known as hexapods with active variable limbs, parallel manipulators have received an increasing interest and attention from the scientific community. Furthermore, potential applications of most parallel manipulators such as multi-axis machine tools, pointing devices, solar panels, radar antennas, telescopes, walking machines, micro manipulators, and so on have found relevant roles in the world of the industry substituting slow, but firmly, at the serial manipulators. An example of the success of parallel manipulators in the industry is the robot Delta, invented by Clavel[4,5] which, in spite of its lower mobility, can performs a wide variety of tasks. On the other hand, it is well known that parallel manipulators based on hexapod architectures makes mechanisms strongly coupled in kinematics, dynamics, and control. Decoupled parallel manipulators are a viable option to overcome such drawbacks.

A decoupled parallel manipulator can be understood in different ways: (i) the position and orientation of the moving platform can be achieved separately by means of different sets of active joints, (ii) not all the active limbs are connected at the moving platform, and (iii) one degree of freedom (DOF) of the moving platform is influenced by only one active joint, the perfect decoupled robot. The first option was investigated by Hunt and Primrose[6] for fully parallel manipulators and was applied by Zlatanov *et al.*[7] in the design of a 6-DOF three-legged parallel manipulator. The second option allows mixed motions over the end-effector or output platform and it is used in this contribution. Furthermore, taking into account that the forward position analysis (FPA) of parallel manipulators with decoupled motions can be easily derived in closed form, Gallardo-Alvarado *et al.*[8] proposed a family of nonoverconstrained redundantly actuated parallel manipulators and Gao *et al.*[9, 10] developed a 5-DOF machine tool. Of course, as it is shown in refs. [11–13], the idea of decoupled motions is also applicable to the so-called defective parallel manipulators, in other words, spatial parallel manipulators with fewer than six DOF. However, these contributions proposed asymmetrical manipulators and in some cases the inclusion of compound joints, or kinematic pairs formed from two or more distinct kinematic pairs, difficult the mechanical assembly and performance of these parallel manipulators. Alternatively, the manipulability and workspace can be increased by connecting a serial manipulator to the moving platform of a parallel manipulator, a natural an evident possibility. For example, a spherical wrist can be attached at the moving platform of a Tricept yielding a 6-DOF spatial mechanism,[14] other combinations were reported in Carbone and Ceccarelli.[15,16] Furthermore, if the spherical wrist is an open chain, then, in order to improve the stiffness, the serial manipulator can be remplazed by a parallel manipulator, producing a serial–parallel manipulator (see, for instance, references).[17–21] However, it is important to mention that a serious drawback of serial–parallel manipulators is that not always is possible to attach the active limbs at the fixed platform, thus the corresponding payload/capacity ratio, a fundamental characteristic of parallel manipulators, could be questionable.

In this work a novel decoupled robot, called LinceJJP, formed from an inner serial–parallel manipulator and an external parallel manipulator, with a common moving platform in which, unlike the contributions of Brodsky *et al.*[22] and Austad,[23] all the active limbs are attached at the fixed platform is introduced.

2. Description of the Robot LinceJJP

A general Gough–Stewart platform is a parallel manipulator composed by a moving platform and a fixed platform connected to each other by means of six variable limbs UPS-type (R, U, P, and S = Revolute, Universal, Prismatic, and

* Corresponding author. E-mail: gjaime@itc.mx

Spherical joint, respectively). The limbs are connected at the fixed platform by means of six distinct universal joints and at the moving platform by means of six distinct spherical joints. Usually, the spherical joints are placed in such a way that form a plane over the moving platform. It is well known that such architecture limits seriously the workspace and manipulability of this mechanism. Furthermore, the FPA, a necessary step in the design process of any mechanism, is a complicated task that leads to a multiple solution due to the coupled motions over the moving platform. In fact, given the limb lengths of this parallel manipulator, the moving platform can reach up to 40 different locations with respect to the fixed platform.[24–26]

In order to overcome the drawbacks, or at least to ameliorate it, of a general Gough–Stewart platform, preserving its merits such as stiffness and accuracy, in this work a new spatial mechanism is presented. The basic idea consists of transforming the general Gough–Stewart platform into a spatial mechanism with decoupled motions over the output platform (see Fig. 1).

Figure 1(a) is a schematic representation of the classical general Gough–Stewart platform. Please note that the six spherical joints attached at the moving platform form a plane and therefore the workspace of the mechanism is seriously affected. In addition, the FPA is a complicated task due to the fact that the pose of the moving platform depends of the coupled displacements of the six limbs. In order to improve the manipulability and to increase the workspace, the spherical joints can be relocated in such a way that two different planes are formed taking two groups of kinematic pairs, where each group contains three spherical joints (Fig. 1(b)). As it is shown in Chen and You,[27] the benefits of this modification are indisputable, however this option cannot eliminate the problem of coupled motions of the six limbs. In order to eliminate this inconvenient, the two planes can be transformed into two moving platforms connected each other by means of three passive variable limbs, preserving the outer active limbs which connects the output platform at the fixed platform (Fig. 1(c)). Several topologies can be derived from this possibility, and only one is studied here.

The robot proposed in this contribution consists of an internal serial–parallel manipulator formed from two serially connected 3-RPS parallel manipulators,[28] and an external 3-UPS parallel manipulator,[1–3,29] (see Fig. 2). As far as the authors are aware, this architecture or topology had not been considered in previous works.

As it is shown in Fig. 2, the architecture of the robot LinceJJP is simple, compact and it is obtained as follows. The robot is composed by two moving platforms, namely the middle platform and the output platform, and a fixed platform. The middle platform is connected at the fixed platform by means of three RPS-type kinematic chains, where the prismatic joints play the role of active joints, and therefore three DOF, one translation, and two rotations are provided to the middle platform with respect to the fixed platform. On the other hand, the output platform is connected at the middle platform by means of three passive RPS-type limbs, whose function is to restrict one rotation of the output platform with respect to the middle platform. Finally, the output platform is connected at the fixed platform by means of three UPS-type kinematic chains, where the prismatic joints play the role of active joints. With this topology all the active variable limbs are, conveniently, attached at the fixed platform.

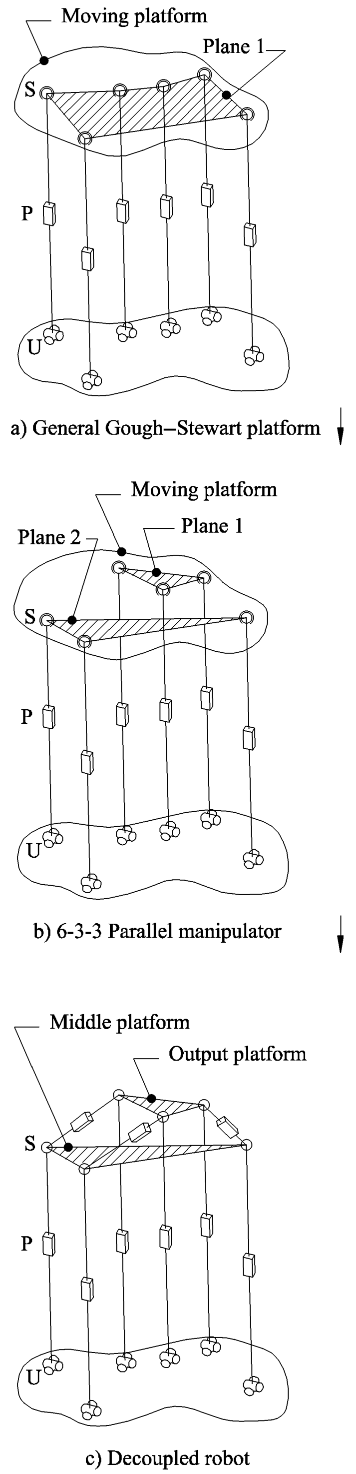

Fig. 1. The transformation of a general Gough–Stewart platform into a decoupled robot.

The idea of using more than one moving platform, of course, is not new. In fact, the trend of using mechanisms formed from serially connected parallel manipulators, also known as hyper redundant manipulators, has been

https://doi.org/10.1017/S0263574709990749 Published online by Cambridge University Press

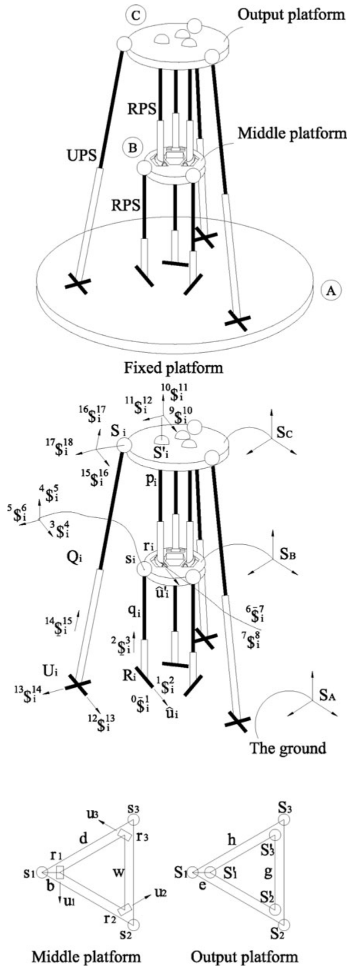

Fig. 2. Robot LinceJJP and its geometric scheme.

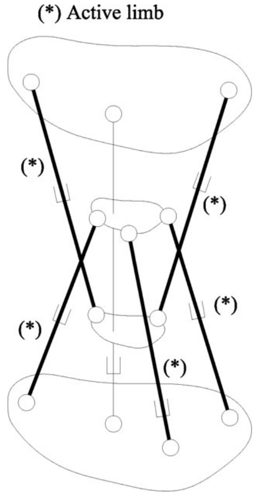

Fig. 3. Arm device of Austad.

extensively reported in the literature.[30–35] However, in such mechanisms not all the active limbs can be attached at the fixed platform. On the other hand, the robot introduced here differs from the double circular-triangular 6-DOF parallel robot proposed by Brodsky *et al.*[22] in that such mechanism is formed with two serially connected 3-DOF planar mechanisms; where each planar mechanism consists of a circular–triangular combination, in which the triangle is connected at the circle by means of three sliders pivoted on axes, with such architecture only three of the six active joints can be attached at the fixed platform. In fact, the design of Brodsky *et al.*[22] requires that active limbs must be attached at the upper moving platform, with its corresponding servos. Similarly, taking into account that the robot patented by Austad[23] (see Fig. 3), is composed of five variable SPS-type limbs and only three of them can be attached at the fixed platform, then one can assume that the robot LinceJJP has a compact topology due to the fact that all the active limbs are connected directly to the fixed platform, simplifying the kinematics and control of it.

Finally, in order to verify the novelty of the proposed robot, the reader is referred to[36–38] where an exhaustive atlas of parallel manipulators as well as constructed prototypes can be consulted.

2.1. Discussion of the mobility of LinceJJP

The correct computation of the effective DOF F in closed chains is an open problem. An exhaustive review of formulae addressing this topic is reported in Gogu.[39] Regarding to the existing methods of computation, these formulae are valid under specific conducted considerations. Clearly, the problem is more complex for mechanisms formed from two or more parallel manipulators, so is the case of hyper-redundant manipulators.

The following is a variant of the well-known Kutzbach–Grübler formula for computing the DOF of spatial parallel manipulators

$$F = 6(n - j - 1) + \sum_{i=1}^{j} f_i, \tag{1}$$

where n is the number of links, j is the number of kinematic pairs, and f_i is the number of freedoms of the ith kinematic pair. For the robot LinceJJP $n = 21$, $j = 6R + 9P + 3U + 9S = 27$, $\sum_{i=1}^{j} f_i = 48$ and therefore $F = 6$. In what follows this apparent correct result is analyzed.

The 3-RPS parallel manipulator was introduced by the first time by Hunt[40] and its kinematic characteristics were extensively investigated, among others, by Huang and coworkers[41–44]. Dai *et al.*[45] proved that in a 3-RPS parallel manipulator a basis representing the motions of the moving platform, with respect to the fixed platform, consists of three elements, two nonparallel coplanar rotations, and one translation along an axis perpendicular to the plane formed by the spherical joints. According to this basis, the middle platform of the robot under study cannot rotate with respect to the fixed platform along an axis perpendicular to the plane formed by the spherical joints attached at the middle platform. It is straightforward to demonstrate that such argument is valid too for the output and middle platforms, in fact, the output platform has a rotation restricted with respect to the middle platform due to the passive 3-RPS parallel manipulator connecting both platforms. With these considerations in mind, although the computed DOF of the robot at hand is six, the output platform does not accept

https://doi.org/10.1017/S0263574709990749 Published online by Cambridge University Press

arbitrary orientations with respect to the fixed platform. Finally, in order to reinforce this conclusion, the following paragraph is an adaptation of interesting comments provided by one of the reviewers.

The screw system describing the kinematics of the middle platform, with respect to the fixed platform, is composed of three screws of zero pitch lying in the plane formed by the centres of the spherical joints attached to the middle platform. Similarly, the screw system describing the kinematics of the output platform, with respect to the middle platform, is composed of three screws of zero pitch lying in the plane formed by the spherical joints attached at the output platform. Therefore, the total composition of the two screw systems should be 6 DOF; however, due to the fact that they intersect, they admit a reciprocal wrench, which is the wrench of infinite pitch orthogonal to the two planes associated to the spherical joints. Due to this, the robot loses 1 DOF.

3. Finite Kinematics

In this section the position analysis of the proposed robot is presented.

3.1. Forward position analysis

The FPA is a crucial step in the design process of parallel manipulators, and for the manipulator robot under study is formulated as follows: Given a set of six generalized coordinates $\{Q_i, q_i\}(i = 1, 2, 3)$, compute the feasible locations that the output platform can reach with respect to the fixed platform.

Due to the decoupled architecture, the pose of the middle platform, body B, with respect to the fixed platform, body A, is controlled by means of the internal generalized coordinates $q_i(i = 1, 2, 3)$. Furthermore, the pose of the middle platform is easily determined through the computation of the coordinates of the centres of the spherical joints attached at the middle platform, points $s_i = (x_i, y_i, z_i)$.

With reference to Fig. 2, the revolute joints attached at the fixed platform impose the following geometric constraints over the middle platform

$$(\boldsymbol{s}_i - \boldsymbol{R}_i) \bullet \hat{\boldsymbol{u}}_i = 0 \quad i = 1, 2, 3, \tag{2}$$

where $\boldsymbol{R}_i$ is the position vector of the nominal point R_i of the ith revolute joint, $\hat{\boldsymbol{u}}_i$ is the axis of the revolute joint, $\boldsymbol{s}_i$ locates the point s_i, and the dot $\bullet$ denotes the usual inner product of the three-dimensional vectorial algebra. Furthermore, three closure equations can be written as

$$(\boldsymbol{s}_i - \boldsymbol{R}_i) \bullet (\boldsymbol{s}_i - \boldsymbol{R}_i) = q_i^2 \quad i = 1, 2, 3. \tag{3}$$

Finally, according to the triangle $s_1 s_2 s_3$ three compatibility equations are given by

$$(\boldsymbol{s}_i - \boldsymbol{s}_j) \bullet (\boldsymbol{s}_i - \boldsymbol{s}_j) = d^2 \quad i, j = 1, 2, 3 \; mod(3) \tag{4}$$

Expressions (2), (3), and (4) represent a system of nine equations in the nine unknowns $x_i, y_i, z_i (i = 1, 2, 3)$ that can be reduced, see for instance references,[46,47] into a univariate 16th polynomial equation. Once the coordinates of the points s_i are calculated, the origin of the reference frame S_B with respect to the fixed reference frame S_A, vector ${}^A\boldsymbol{\rho}^B$, results in

$${}^A\boldsymbol{\rho}^B = (\boldsymbol{s}_1 + \boldsymbol{s}_2 + \boldsymbol{s}_3)/3. \tag{5}$$

Finally, the pose of the middle platform with respect to the fixed platform is summarized in the 4×4 homogeneous transformation matrix ${}^A\mathbf{T}^B$:

$${}^A\mathbf{T}^B = \begin{bmatrix} {}^A\mathbf{R}^B & {}^A\boldsymbol{\rho}^B \\ \mathbf{O}_{1\times 3} & 1 \end{bmatrix}, \tag{6}$$

where ${}^A\mathbf{R}^B$ is the rotation matrix which is computed by means of the coordinates of the points $s_i(i = 1, 2, 3)$, for details see Gallardo-Alvarado *et al.*[48]

Following a similar procedure, the pose of the output platform, with respect to the fixed platform, is computed. This problem consists of finding the coordinates of the centres of the spherical joints attached at the output platform, points $S_i = (X_i, Y_i, Z_i), i = 1, 2, 3,$ given the pose of the middle platform, with respect to the fixed platform, and the generalized coordinates $Q_i(i = 1, 2, 3)$. To this end, consider the following closure equations

$$\left.\begin{array}{l} \boldsymbol{S}_1 + \boldsymbol{S}_2 + \boldsymbol{S}_3 = \boldsymbol{S}'_1 + \boldsymbol{S}'_2 + \boldsymbol{S}'_3, \\ (\boldsymbol{S}'_i - \boldsymbol{r}_i) \bullet \hat{\boldsymbol{u}}'_i = 0, (\boldsymbol{S}_i - \boldsymbol{U}_i) \bullet (\boldsymbol{S}_i - \boldsymbol{U}_i) = Q_i^2, \\ (\boldsymbol{S}_i - \boldsymbol{S}'_i) \bullet (\boldsymbol{S}_i - \boldsymbol{S}'_i) = e^2 (i = 1, 2, 3), \\ (\boldsymbol{S}_i - \boldsymbol{S}_j) \bullet (\boldsymbol{S}_i - \boldsymbol{S}_j) = b^2 \quad i, j = 1, 2, 3 \; mod(3), \\ (\boldsymbol{S}'_i - \boldsymbol{S}'_j) \bullet (\boldsymbol{S}'_i - \boldsymbol{S}'_j) = g^2 \quad i, j = 1, 2, 3 \; mod(3), \end{array}\right\} \tag{7}$$

where $\boldsymbol{S}_i, \boldsymbol{S}'_i, \boldsymbol{U}_i, \boldsymbol{r}_i, (i = 1, 2, 3)$ are position vectors of the points $S_i, S'_i, U_i, r_i, (i = 1, 2, 3)$ associated, respectively, to spherical, universal and revolute joints while $\hat{\boldsymbol{u}}'_i$ is the axis of the ith revolute joint $\boldsymbol{r}_i$. Equations (7) represent a system of 18 equations in the unknowns $X_i, Y_i, Z_i, X'_i, Y'_i, Z'_i (i = 1, 2, 3)$. It is important to emphasize that due to the variable orientation of the middle platform, the procedure to solve (7) is more complicated than the derived for the middle platform. The solution of this kind of equations was successfully approached by Innocenti and Parenti-Castelli.[29]

Finally, once the coordinates $S_i(i = 1, 2, 3)$ is computed, the homogeneous transformation matrix ${}^A\mathbf{T}^C$ between the output and fixed platforms results in

$${}^A\mathbf{T}^C = \begin{bmatrix} {}^A\mathbf{R}^C & {}^A\boldsymbol{\rho}^C \\ \mathbf{O}_{1\times 3} & 1 \end{bmatrix}, \tag{8}$$

where

$${}^A\boldsymbol{\rho}^C = (\boldsymbol{S}_1 + \boldsymbol{S}_2 + \boldsymbol{S}_3)/3 \tag{9}$$

is the geometric centre of the output platform expressed in the reference frame S_A and ${}^A\mathbf{R}^C$ is the rotation matrix between reference frames S_C and S_A. Furthermore, the homogeneous transformation matrix ${}^B\mathbf{T}^C$ between the output and fixed platforms can be calculated from

$${}^A\mathbf{T}^C = {}^A\mathbf{T}^B \; {}^B\mathbf{T}^C. \tag{10}$$

3.2. *Inverse position analysis*

The inverse position analysis consists of finding the limb lengths of the robot given the pose, or transformation matrix ${}^A\mathbf{T}^C$, of the output platform with respect to the fixed platform.

Clearly, the coordinates of any point W attached at the output platform can be obtained as

$$W_{SA} = {}^A\mathbf{R}^C\, W_{SC} + {}^A\boldsymbol{\rho}^C, \tag{11}$$

where W_{SA} is point W expressed in the fixed reference frame S_A while W_{SC} is the same point but expressed in the moving reference frame S_C. The centres of the spherical joints attached at the output platform are computed by means of Eq. (11), after the lengths $Q_i (i = 1, 2, 3)$ result in

$$Q_i^2 = (\boldsymbol{S}_i - \boldsymbol{U}_i) \bullet (\boldsymbol{S}_i - \boldsymbol{U}_i) \quad i = 1, 2, 3. \tag{12}$$

On the other hand, due to the tangential arrangement of the kinematic pairs attached at the middle platform it is possible to write three geometric constraints as

$$\left.\begin{array}{l}(\boldsymbol{S}_1' - \boldsymbol{r}_1) \bullet (\boldsymbol{s}_2 - \boldsymbol{s}_3) = 0, (\boldsymbol{S}_2' - \boldsymbol{r}_2) \bullet (\boldsymbol{s}_3 - \boldsymbol{s}_1) = 0,\\ (\boldsymbol{S}_3' - \boldsymbol{r}_3) \bullet (\boldsymbol{s}_1 - \boldsymbol{s}_2) = 0.\end{array}\right\} \tag{13}$$

Moreover, according to triangles $s_1 s_2 s_3$ and $r_1 r_2 r_3$ one can write

$$\boldsymbol{s}_1 + \boldsymbol{s}_2 + \boldsymbol{s}_3 = \boldsymbol{r}_1 + \boldsymbol{r}_2 + \boldsymbol{r}_3. \tag{14}$$

Furthermore, the variable lengths p_i are restricted to

$$(\boldsymbol{S}_i' - \boldsymbol{r}_i) \bullet (\boldsymbol{S}_i' - \boldsymbol{r}_i) = p_i^2 \tag{15}$$

whereas three compatibility geometric constraints are given by

$$(\boldsymbol{s}_i - \boldsymbol{r}_i) \bullet (\boldsymbol{s}_i - \boldsymbol{r}_i) = b^2 \quad i = 1, 2, 3. \tag{16}$$

Finally, according to the triangle $r_1 r_2 r_3$ it follows that

$$(\boldsymbol{r}_i - \boldsymbol{r}_j) \bullet (\boldsymbol{r}_i - \boldsymbol{r}_j) = w^2 \; i, j = 1, 2, 3 \; mod(3). \tag{17}$$

Equations (2)–(4) and (13)–(17) allow to determine the unknowns $\boldsymbol{r}_i$, $\boldsymbol{s}_i$, p_i, and q_i. At this point it is important to emphasize that, as it was correctly noted by one of the reviewers, the topology of the proposed robot is such that there exist passive translations over the middle platform. The manipulation of such extra DOF allows to improve the dexterity of the hybrid manipulator. Consider for instance that the user has the possibility to assign arbitrary values to one of the generalized coordinates q_i in order to avoid singularities, without affecting the final pose of the output platform.

4. Infinitesimal Kinematics

In this section the velocity and acceleration analyses of the proposed robot are approached by using the theory of screws. For detailed information of the kinematic analysis of closed chains and parallel manipulators, using this mathematical resource, the reader is referred to.[49–52]

The modeling of the screws is depicted in Fig. 2. In order to solve the inverse velocity and acceleration analyses, it is necessary the introduction of auxiliary screws with the purpose to satisfy the required rank of the involved Jacobian matrices, with this consideration in mind the revolute joints are modeled as cylindrical joints, in which the corresponding translational velocities are equal to zero. In other words, ${}_0\overline{\omega}_1{}^i = {}_6\overline{\omega}_7{}^i = 0 (i = 1, 2, 3)$.

4.1. *Velocity analysis*

Let ${}^A\boldsymbol{\omega}^C$ and ${}^A\boldsymbol{v}_O^C$ be, respectively, the angular and linear velocities of a point O attached at the output platform. The velocity state, or twist about a screw, of the output platform with respect to the fixed platform, ${}^A\boldsymbol{V}^C = [{}^A\boldsymbol{\omega}^C, {}^A\boldsymbol{v}_O^C]^T$, can be obtained trough the middle and fixed platforms as

$${}^A\boldsymbol{V}^C = {}^A\boldsymbol{V}^B + {}^B\boldsymbol{V}^C, \tag{18}$$

where ${}^A\boldsymbol{V}^B$ is the velocity state of the middle platform with respect to the fixed platform, and ${}^B\boldsymbol{V}^C$ is the velocity state of the output platform with respect to the middle platform. Furthermore, these kinematic states can be written in screw form as follows

$$\boldsymbol{V} = \mathbf{J}_i \Omega_i, \;\; \boldsymbol{V} \in \{{}^A\boldsymbol{V}^B, {}^B\boldsymbol{V}^C, {}^A\boldsymbol{V}^C\} \quad i = 1, 2, 3, \tag{19}$$

where the Jacobian matrices $\mathbf{J}_i \in \{{}^A\mathbf{J}_i^B, {}^B\mathbf{J}_i^C, {}^A\mathbf{J}_i^C\}$ are given by

$$\begin{aligned}
{}^A\mathbf{J}_i^C &= \left[{}^{12}\overline{\$}_i^{13}, {}^{13}\$_i^{14}, {}^{14}\underline{\$}_i^{15}, {}^{15}\$_i^{16}, {}^{16}\$_i^{17}, {}^{17}\$_i^{18}\right],\\
{}^B\mathbf{J}_i^C &= \left[{}^{6}\overline{\$}_i^{7}, {}^{7}\$_i^{8}, {}^{8}\underline{\$}_i^{9}, {}^{9}\$_i^{10}, {}^{10}\$_i^{11}, {}^{11}\$_i^{12}\right],\\
{}^A\mathbf{J}_i^B &= \left[{}^{0}\overline{\$}_i^{1}, {}^{1}\$_i^{2}, {}^{2}\underline{\$}_i^{3}, {}^{3}\$_i^{4}, {}^{4}\$_i^{5}, {}^{5}\$_i^{6}\right],
\end{aligned}$$

whereas $\Omega_i \in \{{}^A\Omega_i^B, {}^B\Omega_i^C, {}^A\Omega_i^C\}$ are matrices containing the joint velocity rates. In fact:

$$\begin{aligned}
{}^A\Omega_i^C &= \left[{}_{12}\overline{\omega}_{13}^i \; {}_{13}\omega_{14}^i \; {}_{14}\underline{\omega}_{15}^i \; {}_{15}\omega_{16}^i \; {}_{16}\omega_{17}^i \; {}_{17}\omega_{18}^i\right]^T,\\
{}^B\Omega_i^C &= \left[{}_{6}\overline{\omega}_{7}^i \; {}_{7}\omega_{8}^i \; {}_{8}\underline{\omega}_{9}^i \; {}_{9}\omega_{10}^i \; {}_{10}\omega_{11}^i \; {}_{11}\omega_{12}^i\right]^T,\\
{}^A\Omega_i^B &= \left[{}_{0}\overline{\omega}_{1}^i \; {}_{1}\omega_{2}^i \; {}_{2}\underline{\omega}_{3}^i \; {}_{3}\omega_{4}^i \; {}_{4}\omega_{5}^i \; {}_{5}\omega_{6}^i\right]^T.
\end{aligned}$$

The inverse velocity analysis consists of finding the joint velocity rates of the robot given a prescribed velocity state of the output platform with respect to the fixed platform, ${}^A\boldsymbol{V}^C$. This analysis is solved directly by means of expressions (18) and (19), however the lost freedom of the output platform must be taken into proper account in order to obtain the desired velocity state. Furthermore, it is important to emphasize that the Jacobians ${}^A\mathbf{J}_i^B$, ${}^B\mathbf{J}_i^C$, and ${}^A\mathbf{J}_i^C$ must be invertible, otherwise the robot is at singular configuration.

On the other hand, the forward velocity analysis consists of finding the velocity state ${}^A\boldsymbol{V}^C$, given the active joint velocity rates of the robot. It is interesting to note that due to the decoupled architecture, the velocity state ${}^A\boldsymbol{V}^B$ depends only of the three active joints ${}_2\underline{\omega}_3{}^i (i = 1, 2, 3)$. Furthermore, since ${}^3\$_i^4$ and ${}^4\$_i^5$ are reciprocal to the remaining screws representing the revolute joints in the same limbs, the application of the Klein form, $\{*; *\}$, between the velocity state ${}^{A}\boldsymbol{V}^{B}$ and these reciprocal screws, the reduction of terms leads to

$$\underline{\mathbf{J}}_1^T\ \Delta\ {}^{A}\boldsymbol{V}^{B} = [0\ {}_2\underline{\omega}_3^1\ 0\ {}_2\underline{\omega}_3^2\ 0\ {}_2\underline{\omega}_3^3]^T, \qquad (20)$$

where $\underline{\mathbf{J}}_1 = [{}^3\$_1^4, {}^4\$_1^5, {}^3\$_2^4, {}^4\$_2^5, {}^3\$_3^4, {}^4\$_3^5]$ and $\Delta = \begin{bmatrix}\mathbf{O} & \mathbf{I}\\ \mathbf{I} & \mathbf{O}\end{bmatrix}$ is an operator of polarity defined by the 3×3 identity matrix $\mathbf{I}$ and the 3×3 zero matrix $\mathbf{O}$. Henceforth, the velocity state ${}^{A}\boldsymbol{V}^{B}$ is obtained directly from Eq. (20).

In order to compute the velocity state ${}^{A}\boldsymbol{V}^{C}$ please note that the screws ${}^{16}\$_i^{17}(i = 1, 2, 3)$ are reciprocal to the remaining screws, in the same limb, representing the revolute joints of the UPS-type limbs. Thus, after applying the Klein form between these screws and the velocity state ${}^{A}\boldsymbol{V}^{C}$, the reduction of terms yields

$$\left\{{}^{16}\$_i^{17};\ {}^{A}\boldsymbol{V}^{C}\right\} = {}_{14}\underline{\omega}_{15}^{i}\quad i = 1, 2, 3. \qquad (21)$$

Similarly, the application of the Klein form of the screws ${}^{9}\$_i^{10}(i = 1, 2, 3)$ to both sides of Eq. (18) allows to write

$$\left\{{}^{9}\$_i^{10};\ {}^{A}\boldsymbol{V}^{C}\right\} = \left\{{}^{9}\$_i^{10};\ {}^{A}\boldsymbol{V}^{B}\right\}\quad i = 1, 2, 3. \qquad (22)$$

Finally, casting into a matrix–vector form Eqs. (21) and (22) one obtains

$$\underline{\mathbf{J}}_2^T\ \Delta\ {}^{A}\boldsymbol{V}^{C} = \begin{bmatrix} {}_{14}\underline{\omega}_{15}^{1} \\ {}_{14}\underline{\omega}_{15}^{2} \\ {}_{14}\underline{\omega}_{15}^{3} \\ \left\{{}^{9}\$_1^{10};\ {}^{A}\boldsymbol{V}^{B}\right\} \\ \left\{{}^{9}\$_2^{10};\ {}^{A}\boldsymbol{V}^{B}\right\} \\ \left\{{}^{9}\$_3^{10};\ {}^{A}\boldsymbol{V}^{B}\right\} \end{bmatrix}, \qquad (23)$$

where $\underline{\mathbf{J}}_2 = [{}^{16}\$_1^{17}, {}^{16}\$_2^{17}, {}^{16}\$_3^{17}, {}^{9}\$_1^{10}, {}^{9}\$_2^{10}, {}^{9}\$_3^{10}]$. Therefore the velocity state ${}^{A}\boldsymbol{V}^{C}$ can be computed directly from Eq. (23). Please note that the forward velocity analysis requires that the active Jacobian matrices $\underline{\mathbf{J}}_1$ and $\underline{\mathbf{J}}_2$ must be invertible, otherwise the manipulator is at a singular configuration.

In what follows the redundancy of the robot is briefly explained. First, consider that according to subsection 2.1 ${}^{A}\boldsymbol{\omega}^{B} \bullet {}^{A}\boldsymbol{\tau}^{B} = {}^{B}\boldsymbol{\omega}^{C} \bullet {}^{B}\boldsymbol{\tau}^{C} = 0$ where ${}^{A}\boldsymbol{\tau}^{B}$ and ${}^{B}\boldsymbol{\tau}^{C}$ are, respectively, normal vectors to the planes $s_1s_2s_3$ and $S_1S_2S_3$. Furthermore, it is evident that ${}^{A}\boldsymbol{\omega}^{C} = {}^{A}\boldsymbol{\omega}^{B} + {}^{B}\boldsymbol{\omega}^{C}$. Therefore the lost rotation of the robot leads to

$${}^{A}\boldsymbol{\omega}^{C} \bullet ({}^{A}\boldsymbol{\tau}^{B} + {}^{B}\boldsymbol{\tau}^{C}) - {}^{A}\boldsymbol{\omega}^{B} \bullet {}^{B}\boldsymbol{\tau}^{C} - {}^{B}\boldsymbol{\omega}^{C} \bullet {}^{A}\boldsymbol{\tau}^{B} = 0. \qquad (24)$$

Equation (24) is called a *zero-torsion condition* and indicates that one element of the angular velocity ${}^{A}\boldsymbol{\omega}^{C}$ can be written as a linear combination of its remaining components. With this consideration in mind the velocity state ${}^{A}\boldsymbol{V}^{C}$ can be considered, by using a proper reference frame, as a five-dimensional vector which implies that it is possible to write, according to Eqs. (20) and (23), ${}^{A}\boldsymbol{V}^{C}$ in terms of first-order coefficients[53] as

$${}^{A}\boldsymbol{V}^{C} = \mathbf{G}\mathbf{Q} + \mathbf{Q}_{*} \qquad (25)$$

where $\mathbf{Q}$ is a 5×1 matrix containing five of the six generalized or active joint velocity rates which is affected by the 5×5 matrix $\mathbf{G}$ whose elements are the corresponding first order coefficients of the chosen active joints while $\mathbf{Q}_{*}$ is a 5×1 matrix formed with the remaining active joint multiplied by its corresponding first order coefficients. Given a prescribed velocity state ${}^{A}\boldsymbol{V}^{C}$, expression (25) indicates that the user can select five of the six active joints and the remaining one can be used in order to avoid/escape from possible singularities, if any. Furthermore, the extra active joint can be used with the purpose to optimize trajectories. This feature is one of the main benefits of the robot LinceJJP.

4.2. *Acceleration analysis*

Let ${}^{A}\boldsymbol{\alpha}^{C}$ and ${}^{A}\boldsymbol{a}_O^{C}$ be, respectively, the angular and linear accelerations of a point O of the output platform. The reduced acceleration state, or accelerator, of the output platform with respect to the fixed platform, ${}^{A}\boldsymbol{A}^{C} = [{}^{A}\boldsymbol{\alpha}^{C}, {}^{A}\boldsymbol{a}_O^{C} - {}^{A}\boldsymbol{\omega}^{C} \times {}^{A}\boldsymbol{v}_O^{C}]^T$, can be obtained trough the middle and fixed platforms as

$${}^{A}\boldsymbol{A}^{C} = {}^{A}\boldsymbol{A}^{B} + {}^{B}\boldsymbol{A}^{C} + [{}^{A}\boldsymbol{V}^{B}\ {}^{B}\boldsymbol{V}^{C}], \qquad (26)$$

where ${}^{A}\boldsymbol{A}^{B}$ is the accelerator of the middle platform with respect to the fixed platform, ${}^{B}\boldsymbol{A}^{C}$ is the accelerator of the output platform with respect to the middle platform and the brackets $[*\quad *]$ denote the Lie product. Furthermore, these accelerators can be written in screw form as follows:

$$\boldsymbol{A} = \mathbf{J}_i\dot{\Omega}_i + \boldsymbol{\mathcal{L}}_i \quad \boldsymbol{A} \in \{{}^{A}\boldsymbol{A}^{B}, {}^{B}\boldsymbol{A}^{C}, {}^{A}\boldsymbol{A}^{C}\} i = 1, 2, 3, \qquad (27)$$

where $\dot{\Omega}_i \in \{{}^{A}\dot{\Omega}_i^{B}, {}^{B}\dot{\Omega}_i^{C}, {}^{A}\dot{\Omega}_i^{C}\}$ are matrices containing the joint acceleration rates of the corresponding limbs, whereas $\boldsymbol{\mathcal{L}}_i \in \{{}^{A}\boldsymbol{\mathcal{L}}_i^{B}, {}^{B}\boldsymbol{\mathcal{L}}_i^{C}, {}^{A}\boldsymbol{\mathcal{L}}_i^{C}\}$ are composed Lie products given by

$$\left.\begin{aligned} {}^{A}\boldsymbol{\mathcal{L}}_i^{C} &= \sum_{j=12}^{16}\left[{}_j\omega_{j+1}{}^i\ {}^j\$_i^{j+1}\ \sum_{k=j+1}^{17}{}_k\omega_{k+1}{}^i\ {}^k\$_i^{k+1}\right], \\ {}^{B}\boldsymbol{\mathcal{L}}_i^{C} &= \sum_{j=6}^{10}\left[{}_j\omega_{j+1}{}^i\ {}^j\$_i^{j+1}\ \sum_{k=j+1}^{11}{}_k\omega_{k+1}{}^i\ {}^k\$_i^{k+1}\right], \\ {}^{A}\boldsymbol{\mathcal{L}}_i^{B} &= \sum_{j=0}^{4}\left[{}_j\omega_{j+1}{}^i\ {}^j\$_i^{j+1}\ \sum_{k=j+1}^{5}{}_k\omega_{k+1}{}^i\ {}^k\$_i^{k+1}\right]. \end{aligned}\right\} \qquad (28)$$

The inverse acceleration analysis consists of finding the joint acceleration rates of the robot given a prescribed accelerator ${}^{A}\boldsymbol{A}^{C}$. This analysis is carried out by means of expressions (26) and (27). On the other hand the forward acceleration analysis consists of finding the accelerator of the output platform with respect to the fixed platform ${}^{A}\boldsymbol{A}^{C}$ given the active joint acceleration rates of the robot. This analysis is very close to the presented to solve the forward

https://doi.org/10.1017/S0263574709990749 Published online by Cambridge University Press

velocity analysis, therefore only the obtained expressions are included here. The accelerator ${}^A\boldsymbol{A}^B$ can be computed upon the expression

$$\underline{\mathbf{J}}_1^T \,\Delta\, {}^A\boldsymbol{A}^B = \begin{bmatrix} \left\{{}^3\$_1^4;\, {}^A\boldsymbol{\mathcal{L}}_1^B\right\} \\ {}_2\underline{\dot{\omega}}_3^1 + \left\{{}^4\$_1^5;\, {}^A\boldsymbol{\mathcal{L}}_1^B\right\} \\ \left\{{}^3\$_2^4;\, {}^A\boldsymbol{\mathcal{L}}_2^B\right\} \\ {}_2\underline{\dot{\omega}}_3^2 + \left\{{}^4\$_1^5;\, {}^A\boldsymbol{\mathcal{L}}_2^B\right\} \\ \left\{{}^3\$_3^4;\, {}^A\boldsymbol{\mathcal{L}}_3^B\right\} \\ {}_2\underline{\dot{\omega}}_3^3 + \left\{{}^4\$_3^5;\, {}^A\boldsymbol{\mathcal{L}}_3^B\right\} \end{bmatrix}, \tag{29}$$

whereas the accelerator ${}^A\boldsymbol{A}^C$ can be obtained from

$$\underline{\mathbf{J}}_2^T \,\Delta\, {}^A\boldsymbol{A}^C = \begin{bmatrix} {}_{14}\underline{\dot{\omega}}_{15}^1 + \left\{{}^{16}\$_1^{17};\, {}^A\boldsymbol{\mathcal{L}}_1^C\right\} \\ {}_{14}\underline{\dot{\omega}}_{15}^2 + \left\{{}^{16}\$_1^{17};\, {}^A\boldsymbol{\mathcal{L}}_2^C\right\} \\ {}_{14}\underline{\dot{\omega}}_{15}^3 + \left\{{}^{16}\$_1^{17};\, {}^A\boldsymbol{\mathcal{L}}_3^C\right\} \\ \left\{{}^9\$_1^{10};\, {}^A\boldsymbol{A}^B + [{}^A\boldsymbol{V}^B\ {}^B\boldsymbol{V}^C] + {}^B\boldsymbol{\mathcal{L}}_1^C\right\} \\ \left\{{}^9\$_2^{10};\, {}^A\boldsymbol{A}^B + [{}^A\boldsymbol{V}^B\ {}^B\boldsymbol{V}^C] + {}^B\boldsymbol{\mathcal{L}}_2^C\right\} \\ \left\{{}^9\$_3^{10};\, {}^A\boldsymbol{A}^B + [{}^A\boldsymbol{V}^B\ {}^B\boldsymbol{V}^C] + {}^B\boldsymbol{\mathcal{L}}_3^C\right\} \end{bmatrix}. \tag{30}$$

Finally, please note that the computation of the accelerator ${}^A\boldsymbol{A}^C$, by means of expression (30), does not require the values of the passive joint acceleration rates of the robot.

5. Simulations using ADAMS©

With the purpose to illustrate the functionality of the proposed robot, in this section the robot LinceJJP is used as a 5-DOF parallel kinematic machine tool for milling and drilling operations. To this end, the simulation is carried out using special commercially available software like ADAMS©. Four prescribed trajectories are assigned to the tool tip as follows:

(1) The tool tip performs a translational rectilinear displacement from point (0,−1.485,0) to point (0.508,−1.016,−0.254) in such a way that the spindle platform moves with a fixed orientation with respect to the fixed platform.
(2) The tool tip is restricted to move on a semicircle of radius 0.254 located in the XY plane.
(3) The tool tip describes a full circle of radius 0.254 in the XZ plane, with a fixed orientation of the output platform with respect to the fixed platform.
(4) The LinceJJP is proved as a simple drilling machine tool.

These tasks were successfully performed with ADAMS© and they are summarized in Fig. 4. It is important to mention that in this section only five of the six active joints were required.

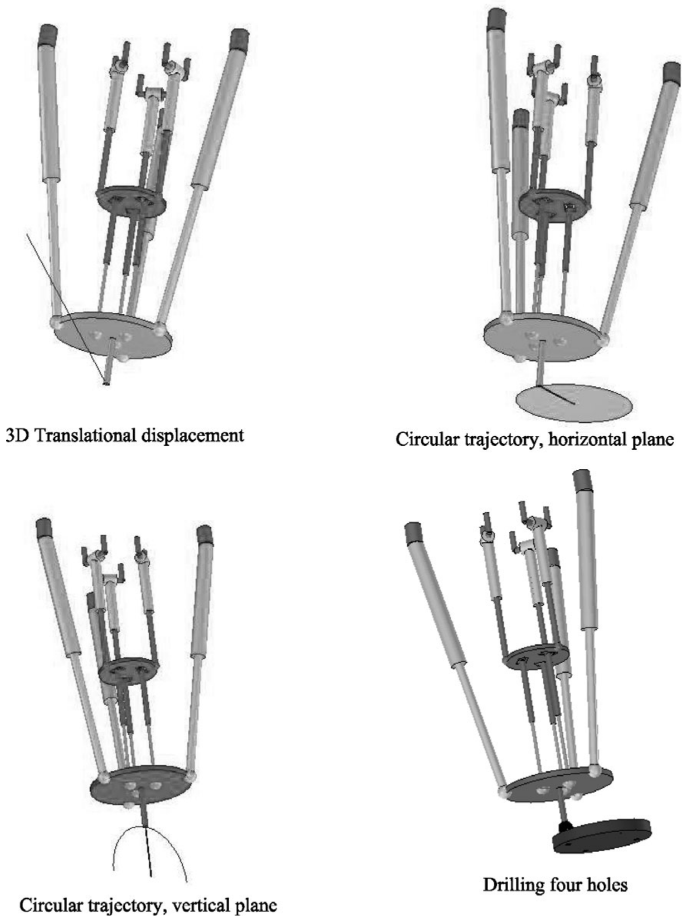

Fig. 4. The robot LinceJJP working as a versatile multi-axis machine tool.

6. Conclusions

In this work a new nonoverconstrained decoupled redundant robot called LinceJJP is presented. As far as the authors are aware this type of architecture has not been considered in previous works. The main features of LinceJJP are:

- Symmetry, a design criterion introduced in robot kinematics by Gosselin and Angeles[54]
- Free of compound joints. In other words, the kinematic joints are placed at different locations.
- Decoupled architecture. Only three of the six active limbs connect the output and fixed platforms.
- A semiclosed form solution is systematically obtained to solve the FPA, a challenging task of most parallel manipulators.
- The proposed robot does not require of special conditions of mechanical assembly in order to satisfy the intersection of screws, and therefore it can be considered as a nonoverconstrained spatial mechanism.
- The six active limbs are attached at the fixed platform, simplifying the kinematics and control of the robot.
- Redundancy. An extra DOF which can be used with the purpose to avoid/escape from singular configurations, as well to optimize trajectories, is available for the proposed robot. Furthermore, any of the six active joints can play this role.

Due to these characteristics LinceJJP is a viable option for practical applications such as redundant multi-axis machine tools, telescopes, radar antennas, solar panels, and so on. Finally, by means of special software like ADAMS©,

https://doi.org/10.1017/S0263574709990749 Published online by Cambridge University Press

LinceJJP is simulated as a five-DOF redundant parallel kinematic machine tool.

Acknowledgment

This work was supported by National Council of Science and Technology of México, Conacyt.

References

1. V. E. Gough, "Contribution to Discussion to Papers on Research in Automobile Stability and Control and in Type Performance," *Proceedings Automation Division Institution of Mechanical Engineers* (1957) pp. 392–395.
2. V. E. Gough and S. G. Whitehall, "Universal Tyre Testing Machine," *Proceedings of the FISITA Ninth International Technical Congress*, IMechE 1, London, UK (1962) pp. 117–137.
3. D. Stewart, "A platform with six degrees of freedom," *Proc. Inst. Mech. Eng. I* **180**(15), 371–386 (1965).
4. R. Clavel, Conception d'un robot parallle rapide 4 degrs de libert *Ph.D. Thesis* (Lausanne, Switzerland: EPFL, 1991).
5. R. Clavel, "Device for the movement and positioning of an element in space," US Patent No. 4,976,582 (Dec. 11, 1990).
6. K. H. Hunt and E. J. F. Primrose, "Assembly configurations of some in-parallel-actuated manipulators," *Mech. Mach. Theory* **28**(1), 31–42 (1993).
7. D. Zlatanov, M. Q. Dai, E. G. Fenton and B. Benhabib, "Mechanical design and kinematic analysis of a three-legged six degree-of-freedom parallel manipulator," *Proc. ASME Robot. Spatial Mech. Mech. Syst. Conf.* **45**, 529–36 (1992).
8. J. Gallardo-Alvarado, G. Alici, L. Pérez-González, "A new family of constrained redundant parallel manipulators," *Multibody Syst. Dyn.*, (Sep. 30, 2009), doi:10.1007/s11044-009-9174-2.
9. F. Gao, B. Peng, W. Li and H. Zhao, "Design of a novel 5-DOF fully parallel kinematic machine tool based on workspace," *Robotica* **23**(1), 35–43 (2005).
10. F. Gao, B. Peng, H. Zhao and W. Li, "A novel 5-DOF fully parallel kinematic machine tool," *Int. J. Adv. Manufact. Tech.* **31**(1–2), 201–207 (2006).
11. J. Gallardo-Alvarado, J. M. Rico-Martínez and G. Alici, "Kinematics and singularity analyses of a 4-dof parallel manipulator using screw theory," *Mech. Mach. Theory* **41**(9), 1048–1061 (2006).
12. J. Gallardo-Alvarado, H. Orozco-Mendoza and A. Maeda-Sánchez, "Acceleration and singularity analyses of a parallel manipulator with a particular topology," *Meccanica* **42**(3), 223–238 (2007).
13. J. Gallardo, R. Rodríguez, M. Caudillo and J. M. Rico, "A family of spherical parallel manipulators with two legs," *Mech. Mach. Theory* **43**(2), 201–216 (2008).
14. C. Innocenti and P. Wenger, "Position Analysis of the RRP-3(SS) Multiloop Spatial Structure," *Proceedings of DETC'04 ASME 2004 Design Engineering Technical Conferences and Computers and Information in Engineering Conference*, Salt Lake City, UT (2004) paper DETC2004-57382 CD-ROM format.
15. G. Carbone and M. Ceccarelli, "A serial–parallel robotic architecture for surgical tasks," *Robotica* **23**(03), 345–354 (2005).
16. G. Carbone and M. Ceccarelli, "A stiffness analysis for a hybrid parallel-serial manipulator," *Robotica* **22**(5), 567–576 (2005).
17. T. K. Tanev, "Kinematics of a hybrid (parallel–serial) robot manipulator," *Mech. Mach. Theory* **35**(9), 1183–1196 (2000).
18. X. Z. Zheng, H. Z. Bin and Y. G. Luo, "Kinematic analysis of a hybrid serial–parallel manipulator," *Int. J. Adv. Manufact. Tech.* **23**(11–12), 925–930 (2004).
19. J. Gallardo-Alvarado, "Kinematics of a hybrid manipulator by means of screw theory," *Multibody Syst. Dyn.* **14**(3–4), 345–366 (2005).
20. Y. Lu and T. Leinonen, "Solution and simulation of position-orientation for multi-spatial 3-RPS parallel mechanisms in series connection," *Multibody Syst. Dyn.* **14**(1), 47–60 (2005).
21. Y. Lu and B. Hu, "Solving driving forces of 2(3-SPR) serial–parallel manipulator by CAD variation geometry approach," *ASME J. Mech. Des.* **128**(6), 1349–1351 (2006).
22. V. Brodsky, D. Glozman and M. Shoham, "Double Circular-Triangular Six Degrees-of-Freedom Parallel Robot," *Sixth International Symposium on Advances in Robot Kinematics,* Salzburg, Austria (1998) pp. 155–164.
23. A. Austad, "Arm device," IPN number WO 87,03239 (Jun. 4, 1987).
24. M. Raghavan, "The Stewart platform of general geometry has 40 configurations," *ASME J. Mech. Des.* **115**(2), 277–282 (1993).
25. C. Innocenti, "Forward Kinematics in Polynomial Form of the General Stewart Platform," *Proceedings ASME 25th Biennial Mechanisms Conference,* Atlanta, GA (1998) pp. 1–10. CD-ROM Paper DETC98/MECH-5894.
26. L. Rolland, "Certified solving of the forward kinematics problem with an exact algebraic method for the general parallel manipulator," *Adv. Robot.* **19**(9), 995–1025 (2005).
27. S. L. Chen and I. T. You, "Kinematic and singularity analyses of a six DOF 6-3-3 parallel link machine tool," *Int. J. Adv. Manufact. Tech.* **16**(11), 835–842 (2000).
28. K. H. Hunt, "Structural kinematics of in-parallel actuated robot arms," *ASME J. Mech. Transm. Auto. Des.* **105**(4), 705–712 (1983).
29. C. Innocenti and V. Parenti-Castelli, "Direct position analysis of the Stewart platform mechanism," *Mech. Mach. Theory* **25**(6), 611–621 (1990).
30. J. S. Pettinato and H. E. Stephanou, "Manipulability and Stability of a Tentacle Based Robot Manipulator," *Proceedings of the IEEE International Conference on Robotics and Automation*, Scottsdale, AZ (1989) pp. 458–63.
31. E. Paljug, T. Ohm and S. Hayati, "The JPL Serpentine Robot: A 12-DOF System for Inspection," *Proceedings of the IEEE International Conference on Robotics and Automation,* Nagoya, Japan (1995) pp. 3143–3148.
32. G. Chirikjian, A. Pamecha and I. Ebert-Uphoff, "Evaluating efficiency of self-reconfiguration in a class of modular robots," *J. Robot. Syst.* **13**(5), 317–338 (1996).
33. K. J. Kyriakopoulos, G. Migadis and K. Sarrigeorgidis, "The NTUA snake: Design, planar kinematics, and motion planning," *J. Robot. Syst.* **16**(1), 37–72 (1999).
34. M. W. Hanan and I. A. Walker, "Kinematics and the implementation of an elephant's trunk manipulator and other continuum style robots," *J. Robot. Syst.* **20**(2), 45–63 (2003).
35. L. Yanming, M. Peisun, Q. Changjun, G. Xueguan, W. Jianbin and Z. Haihong, "Design and study of a novel hyper-redundant manipulator," *Robotica* **21**(5), 505–509 (2003).
36. J.-P. Merlet, website http://www-sop.inria.fr/coprin/equipe/merlet/merlet-eng.html
37. I. Bonev, website http://www.parallemic.org/
38. R. Di Gregorio, "A New Decoupled Parallel Manipulator." *Proceedings of the 10th International Workshop on Robotics in Alpa-Adria-Danube Region*, RAAD 2001, Vienna, Austria (2001) pp. 1–9.
39. G. Gogu, "Mobility of mechanisms: a critical review," *Mech. Mach. Theory* **40**(9), 1068–1097 (2005).
40. K. H. Hunt, "Structural kinematics of in-parallel-actuated robot arms," *ASME J. Mech. Transm. Auto. Des.* **105**, 705–712 (1983).
41. Z. Huang and Y. F. Fang, "Kinematic characteristics analysis of 3 DOF in-parallel actuated pyramid mechanism," *Mech. Mach. Theory* **31**(8), 1009–1018 (1996).
42. Z. Huang and J. Wang, "Instantaneous Motion Analysis of Deficient-Rank 3-DOF Parallel Manipulator by Means of Principal Screws," *Proceedings of A Symposium Commemorating the Legacy, Works, and Life of Sir Robert Stawell Ball Upon the 100th Anniversary of a Treatise on the*

Theory of Screws, University of Cambridge, Trinity College, Cambridge, Cambridgeshire, UK (2000) pp. 1–13.

43. Z. Huang and J. Wang, "Identification of principal screws of 3-DOF parallel manipulators by quadric degeneration," *Mech. Mach. Theory* **36**(8), 893–911 (2001).
44. Z. Huang, J. Wang and Y. Fang, "Analysis of instantaneous motions of deficient-rank 3- RPS parallel manipulators," *Mech. Mach. Theory* **37**(2), 229–240 (2002).
45. J. S. Dai, Z. Huang and H. Lipkin, "Mobility of overconstrained parallel mechanisms," *ASME J. Mech. Des.* **128**(1), 220–229 (2006).
46. L.-W. Tsai, *Robot Analysis* (John Wiley & Sons: New York, 1999).
47. J. Gallardo, H. Orozco, R. Rodríguez and J. M. Rico, "Kinematics of a class of parallel manipulators which generates structures with three limbs," *Multibody Syst. Dyn.* **17**(1), 27–46 (2007).
48. J. Gallardo-Alvarado, C. R. Aguilar-Nájera, L. Casique-Rosas, L. Pérez-González and J. M. Rico-Martínez, "Solving the kinematics and dynamics of a modular spatial hyper-redundant manipulator by means of screw theory," *Multibody Syst. Dyn.* **20**(4), 307–325 (2008).
49. J. M. Rico and J. Duffy, "An application of screw algebra to the acceleration analysis of serial chains," *Mech. Mach. Theory* **31**(4), 445–457 (1996).
50. J. M. Rico, J. Gallardo and J. Duffy, "Screw theory and higher order kinematic analysis of open serial and closed chains," *Mech. Mach. Theory* **34**(4), 559–586 (1999).
51. J. M. Rico and J. Duffy, "Forward and inverse accceleration analyses of in-parallel manipulators," *ASME J. Mech. Des.* **122**(3), 299–303 (2000).
52. J. Gallardo, J. M. Rico, A. Frisoli, D. Checcacci and M. Bergamasco, "Dynamics of parallel manipulators by means of screw theory," *Mech. Mach. Theory* **38**(11), 1113–1131 (2003).
53. J. Gallardo-Alvarado and J. M. Rico-Martínez, "Jerk influence coefficients, via screw theory, of closed chains," *Meccanica* **36**(2), 213–228 (2001).
54. C. M. Gosselin and J. Angeles, "The optimum kinematic design of a spherical three-degree-of-freedom parallel manipulator," *ASME J. Mech. Transm. Auto. Des.* **111**(2), 202–207 (1989).